Journal of Neuro-Oncology (2024) 169:445–455
https://doi.org/10.1007/s11060-024-04747-7

CASE STUDY

Prognostic significance of MRI contrast enhancement in newly diagnosed glioblastoma, IDH-wildtype according to WHO 2021 classification

Alexandre Roux[1,2] · Angela Elia[1,2] · Benoit Hudelist[1] · Joseph Benzakoun[2,3] · Edouard Dezamis[1] · Eduardo Parraga[1] · Alessandro Moiraghi[1,2] · Giorgia Antonia Simboli[1,4] · Fabrice Chretien[2,4] · Catherine Oppenheim[2,3] · Marc Zanello[1,2] · Johan Pallud[1,2]

Received: 9 May 2024 / Accepted: 11 June 2024 / Published online: 24 June 2024

Abstract

Background and objectives Contrast enhancement in glioblastoma, *IDH*-wildtype is common but not systematic. In the era of the WHO 2021 Classification of CNS Tumors, the prognostic impact of a contrast enhancement and the pattern of contrast enhancement is not clearly elucidated.

Methods We performed an observational, retrospective, single-centre cohort study at a tertiary neurosurgical oncology centre (January 2006 - December 2022). We screened adult patients with a newly-diagnosed glioblastoma, *IDH*-wildtype in order to assess the prognosis role of the contrast enhancement and the pattern of contrast enhancement.

Results We included 1149 glioblastomas, *IDH*-wildtype: 26 (2.3%) had a no contrast enhancement, 45 (4.0%) had a faint and patchy contrast enhancement, 118 (10.5%) had a nodular contrast enhancement, and 960 (85.5%) had a ring-like contrast enhancement. Overall survival was longer in non-contrast enhanced glioblastomas (26.7 months) than in contrast enhanced glioblastomas (10.9 months) ($p < 0.001$). In contrast enhanced glioblastomas, a ring-like pattern was associated with shorter overall survival than in faint and patchy and nodular patterns (10.0 months versus 13.0 months, respectively) ($p = 0.033$). Whatever the presence of a contrast enhancement and the pattern of contrast enhancement, surgical resection was an independent predictor of longer overall survival, while age ≥ 70 years, preoperative KPS score < 70, tumour volume $\geq 30 cm^3$, and postoperative residual contrast enhancement were independent predictors of shorter overall survival.

Conclusion A contrast enhancement is present in the majority (97.7%) of glioblastomas, *IDH*-wildtype and, regardless of the pattern, is associated with a shorter overall survival. The ring-like pattern of contrast enhancement is typical in glioblastomas, *IDH*-wildtype (85.5%) and remains an independent predictor of shorter overall survival compared to other patterns (faint and patchy and nodular).

Keywords Magnetic Resonance Imaging · Contrast enhancement · Glioblastoma · Neurosurgery · Survival analysis

Introduction

Glioblastoma, *isocitrate dehydrogenase (IDH)* wildtype (World Health Organization (WHO) grade 4) is the most common malignant primary brain tumour in adults with the worse prognosis [1]. Maximal safe resection [2–7] followed by standard chemoradiotherapy protocol [8] is the current standard of care. At imaging discovery, glioblastoma, *IDH*-wildtype typically present with a ring-like pattern of contrast enhancement (CE) area surrounding central necrosis. The presence of a CE is linked to the presence of a microvascular proliferation or to a blood-brain barrier disruption

Marc Zanello and Johan Pallud participated equally.

✉ Alexandre Roux
alexandre.roux@neurochirurgie.fr

1 Service de Neurochirurgie, GHU-Paris Psychiatrie et Neurosciences, Site Sainte Anne, 1, rue Cabanis, Paris Cedex 14 F-75014, France

2 Institute of Psychiatry and Neuroscience of Paris (IPNP), Université Paris Cité, INSERM U1266, IMA-Brain, Paris F-75014, France

3 Service de Neuroradiologie, GHU Paris Psychiatrie et Neurosciences, Site Sainte Anne, Paris F- 75014, France

4 Service de Neuropathologie, GHU Paris Psychiatrie et Neurosciences, Site Sainte-Anne, Paris F- 75014, France

and is a hallmark for higher-grade diffuse gliomas, which are characterized by neoangiogenesis [9]. In a recent study, the authors demonstrated that the presence of CE and that the pattern of CE (absence, faint and patchy, nodular, and ring-like) significantly impacted survival of diffuse astrocytomas [9]. This highlighted its usefulness as an easily available prognostic marker in an integrated grading system [9]. However, literature on this topic is contradictory and difficult to compare, mainly due to differences in MRI techniques and imaging evaluation criteria, and to variations of tumour classification over time [10–13]. To diagnose a glioblastoma, *IDH*-wildtype in adults, the current 2021 WHO Classification of Tumours of the Central Nervous System does not incorporate the preoperative MRI analysis, and especially the pattern of CE. Several glioblastomas, *IDH*-wildtype, do not exhibit CE and have a radiological appearance that more closely resembles the classic radiological appearance of a lower-grade glioma [14]. However, CE on MRI reflects macroscopically the degree of aggressiveness of a tumour and, therefore, may help refining prognosis [9, 15]. If the presence of a CE helps grading diffuse astrocytomas according to the 2016 WHO Classification, there is no information of its prognostic significance in the specific subgroup of glioblastoma, *IDH*-wildtype according to the current 2021 WHO Classification. Numerous studies have been conducted on the prognostic impact of contrast enhancement in high-grade gliomas. However, few of them focused on a homogeneous population of glioblastomas, IDH-wildtype and, each time, included a small number of cases. Pons-Escoda et al. in 2024, summarized the importance of the pre-operative MRI analysis in the diagnosis of gliomas of any grade taking into account the new WHO 2021 classification and especially the radiological differences between typical glioblastomas, *IDH*-wildtype and molecular ones [16].

In the present study, we assessed the prognostic significance of CE and of the pattern of CE in adult patients harbouring a newly-diagnosed supratentorial glioblastoma, *IDH*-wildtype.

Methods

Study design

An observational, retrospective, single-centre cohort study was conducted at a tertiary neurosurgical oncology centre between January 2006 and December 2022 at the standard chemoradiotherapy protocol era and before the tumor-treating field era [8, 17]. The manuscript was written according to the Strengthening the Reporting of Observational Studies in Epidemiology (STROBE) checklist [18].

Participants

Inclusion criteria were: (1) histo-molecular diagnosis of glioblastoma, *IDH*-wildtype according to the 2021 WHO Classification [1]; (2) available pre- and postoperative MRIs; and (3) available postoperative follow-up. Exclusion criteria were: (1) other histo-molecular subtypes; (2) lack of clinical, imaging and/or follow-up data; and (3) patients under 18 years.

Data collection

Data were systematically gathered from medical records using a protocol designed for the study by the first author (AR). Clinical characteristics at the time of histo-molecular diagnosis were: sex, age, and Karnofsky Performance Status (KPS) score.

Imaging characteristics on preoperative MRI were evaluated on 3D gradient-echo T1 sequence and Fluid-Attenuated with Inversion Recovery (FLAIR) sequence acquired in axial plane or 3D volume. The MRI protocols are detailed in the supplementary materials. The following variables were assessed: presence of CE, pattern of CE (absence, faint and patchy, nodular-like, or ring-like surrounding a central necrosis, as previously described [19]), and tumour volume (i.e. volume of the enhancement and central necrosis, obtained by lesion segmentation on preoperative 3D T1-weighted sequences with gadolinium based on a methodology previously described) [20]. Briefly, one evaluator segmented glioblastoma components on preoperative images with use of open-source Multi-Image Analysis GUI software (2016, MANGO software, version 4.0.1; Research Imaging Institute, University of Texas Health Science Center, San Antonio, http://ric.uthscsa.edu/mango/) and designed several semiautomated scripts from the macro command. We summed enhancing and necrotic components to form the whole solid tumor component, which constituted the subsequent region of interest [20]. Although no central imaging review was performed for all patients for the purpose of the present study, 535 cases (46.6%) cases had previously been centrally reviewed in the framework of previous studies. For these cases, imaging data were obtained from an independent central radiological review by one neuroradiologist while blind to clinical, histopathological, and molecular reviews, and outcomes. Imaging data included: presence of a tumoral CE on preoperative MRI and the pattern of CE (faint and patchy, nodular, and ring-like).

Treatment-related characteristics were: surgical treatment (biopsy versus surgical resection), extent of surgical resection (partial resection defined by removal of < 90% of enhancing tumour, subtotal resection defined by removal of 90–99% of enhancing tumour and total resection defined by

removal of 100% of enhancing tumour [21, 22]), completion of the standard chemoradiotherapy protocol (defined as ≥ 6 cycles of adjuvant Temozolomide). We established the extent of resection by quantifying the volume of residual tumoral contrast enhancement on postoperative (within 48 h) 3D T1-weighted fast spoiled gradient-recalled images. Long-term survivors were defined as patients alive ≥ 2 years since diagnosis.

Table 1 Main characteristics of the study sample ($n = 1149$)

Parameters	Whole series patients ($n = 1149$)	
	n	%
Clinical characteristics		
Sex		
Male	487	42.4
Female	662	57.6
Age		
<70 years	806	70.1
≥70 years	343	29.9
Preoperative Karnofsky Performance Status score		
≥70	870	75.7
<70	279	24.3
Imaging characteristics		
Contrast enhancement		
No	26	2.3
Yes	1123	97.7
Pattern of contrast enhancement		
No	26	2.3
Faint and patchy	45	3.9
Nodular	118	10.3
Ring-like surrounding necrosis	960	83.5
Volume of the CE (cm^3)		
<30 cm^3	594	51.7
≥30 cm^3	555	48.3
Treatment-related characteristics		
Surgical treatment		
Biopsy	534	46.5
Surgical resection	615	53.5
Extent of surgical resection (for CE glioblastomas, n = 1123)		
Biopsy	519	46.2
Partial resection	101	9
Subtotal resection	103	9.2
Total and supratotal resection	400	35.6
Completion of standard radiochemotherapy protocol (n = 1114)		
No	522	46.9
Yes	592	53.1
Survival characteristics		
Long-term survivors		
No	955	83.1
Yes	194	16.9

CE: contrast enhancement

Histomolecular diagnosis

The histological diagnosis of glioblastoma was done when microvascular proliferation or tumor necrosis were detected. Screening for *IDH1* mutations was systematically carried out using immunohistochemistry targeting the *IDH1R132H* mutation. For patients < 55 years old, a targeted DNA-sequencing of *IDH1/2* mutations had additionally been performed to identify minor *IDH* mutations. For patients with an *IDH*-wildtype diffuse astrocytoma lacking histological features of glioblastoma, further molecular analyses were performed to identify molecular signatures of glioblastoma: *EGFR* amplification, combined gain of chromosome 7 and loss of chromosome 10, and/or *hTERT* promoter mutation [1].

Statistical analyses

Continuous variables were described as mean ± standard deviation. Categorical variables were described as percentages. Univariable analyses were carried out, computing unadjusted odds ratios, and using the chi-square or Fisher's exact test for comparing categorical variables, and the unpaired t-test or Mann–Whitney U test for continuous variables, as appropriate. Unadjusted survival curves for overall survival (OS) and progression-free survival (PFS) were plotted by the Kaplan-Meier method, using log-rank tests to assess significance for group comparison. Cox proportional hazard models were constructed using a backward stepwise approach, adjusting for predictors previously associated at the $p < 0.2$ level with mortality and recurrence in unadjusted analysis. We retained only the variables significant at the $p < 0.05$ level. Statistical analyses were performed using JMP software (Version 17.2.0; SAS Institute Inc, Cary, North Carolina, USA).

Results

Clinical, imaging, and treatment-related characteristics

Patient characteristics are detailed in Table 1. The agreement rate of the central imaging review of the 535 cases was 99.3% ($n = 531/535$). The four discordant cases were classified as non-contrast enhanced glioblastomas after review. We included 1149 patients treated for a newly diagnosed supratentorial glioblastoma, *IDH*-wildtype (662 men; mean age of 62 ± 12 years, range 19–93). Twenty-six patients (2.3%) had a non-contrast enhanced glioblastoma, and 1123 patients (97.7%) had a contrast enhanced glioblastoma: 45 faint and patchy CE (4.0%), 118 nodular CE (10.5%),

and 960 ring-like CE surrounding central necrosis (85.5%) (Table 1). The different CE patterns are illustrated in Fig. 1. For all the non-contrast enhanced tumour cases, we confirmed the diagnosis by identifying the molecular features of glioblastoma: *EGFR* amplification, combined gain of chromosome 7 and loss of chromosome 10, and/or *hTERT* promoter mutation. We found a significant higher rate of long-term survivor in the non-contrast enhanced glioblastoma than in patients with a contrast enhanced glioblastoma (42.3% versus 16.3%, respectively) ($p=0.002$). Adjuvant oncological treatment was available for 1114 cases (97.0%) and the completion of the standard chemoradiation protocol was done in 592 cases (53.1%). The median time to start chemoradiation therapy was 6 weeks (mean 5.8 weeks +/- 2.3 weeks).

Survival analyses

During the follow-up period (median,10.2 months; range, 0-141), 1047 patients (91.1%) died and 1087 patients (94.6%) experienced disease progression.

In the whole series, the median PFS was 6.5 months (95%CI, 6.0–7.0). The median PFS was significantly higher in patients with a non-contrast enhanced glioblastoma (9.5 months; 95%CI, 7.0–26.0) than in patients with a contrast enhanced glioblastoma (6.5 months; 95%CI, 6.0–7.0; $p=0.007$) (Supplementary Fig. 1A). In the subgroup of patients with a contrast enhanced glioblastoma ($n=1123$, 97.7%), the median PFS did not significantly differ between faint and patchy CE (7.5 months; 95%CI, 5.0–10.0), nodular CE (7.0 months; 95%CI, 5.5–8.5), and ring-like CE surrounding central necrosis (6.4 months; 95%CI, 6.0–7.0; $p=0.606$) (Supplementary Fig. 1B). The median PFS did not significantly differ between ring-like CE surrounding central necrosis (6.4 months; 95%CI, 6.0–7.0) and other patterns of CE (7.0 months; 95%CI, 6.0-8.5; $p=0.294$) (Supplementary Fig. 1C). After adjustments using Cox models, surgical resection (aHR, 0.59 [95% CI 0.50–0.70], $p<0.001$) was independently associated with a longer PFS, while age ≥ 70 years (aHR, 1.22 [95% CI 1.07–1.40], $p=0.004$), preoperative KPS score < 70 (aHR, 1.48 [95% CI 1.29–1.71], $p<0.001$), tumour volume ≥ 30cm^3 (aHR, 1.27 [95% CI 1.12–1.44], $p<0.001$), and post-operative residual CE (aHR, 1.37 [95% CI 1.15–1.63], $p<0.001$) were independently associated with a shorter PFS (Supplementary Table 1). After adjustments using Cox models in the subgroup of patients with a contrast enhanced glioblastoma, surgical resection (aHR, 0.58 [95% CI 0.49–0.69], $p<0.001$) was independently associated with a longer PFS, while age ≥ 70 years (aHR, 1.23 [95% CI 1.08–1.41], $p=0.003$), preoperative KPS score < 70 (aHR, 1.49 [95% CI 1.29–1.72], $p<0.001$), tumour volume ≥ 30cm^3 (aHR, 1.27 [95% CI 1.12–1.44], $p<0.001$), and post-operative residual CE (aHR, 1.35 [95% CI 1.13–1.61], $p=0.001$) were independently associated with a shorter PFS (Supplementary Table 2).

Fig. 1 Illustrative cases
MRI illustration with 3 sequences (T1-weighted, T1-weighted with gadolinium injection and FLAIR). **(Upper left)** glioblastoma *IDH*-wildtype without CE. **(Upper right)** glioblastoma *IDH*-wildtype with a faint and patchy CE. **(Lower left)** glioblastoma *IDH*-wildtype with a nodular CE. **(Lower right)** glioblastoma *IDH*-wildtype with a ring-like CE surrounding central necrosis

In the whole series, the median OS was 11.0 months (95%CI, 10.0–12.0). The median OS was significantly higher in patients with a non-contrast enhanced glioblastoma (26.7 months; 95%CI, 16.0-30.5) than in patients with a contrast enhanced glioblastoma (10.9 months; 95%CI, 10.0–12.0; $p<0.001$) (Fig. 2A). In the subgroup of patients with a contrast enhanced glioblastoma ($n=1123$, 97.7%), the median OS did not significantly differ between faint and patchy CE (12.5 months; 95%CI, 7.5–17.7), nodular CE (13.0 months; 95%CI, 10.7–16.5), and ring-like CE (10.0 months; 95%CI, 9.4–11.2; $p=0.071$) (Fig. 2B). The median OS was significantly shorter in ring-like CE surrounding central necrosis (10.0 months; 95%CI, 9.4–11.2) than in other patterns of CE (13.0 months; 95%CI, 11.0-16.2; $p=0.033$) (Fig. 2C). After adjustments using Cox models, surgical resection (aHR, 0.53 [95% CI 0.45–0.64], $p<0.001$) was independently associated with a longer OS, while age ≥ 70 years (aHR, 1.47 [95% CI 1.28–1.69], $p<0.001$), preoperative KPS score < 70 (aHR, 1.72 [95% CI 1.48–1.99], $p<0.001$), presence of a CE whatever the CE pattern (aHR, 1.81 [95% CI 1.12–2.94], $p=0.015$), tumour volume ≥ 30cm^3 (aHR, 1.44 [95% CI 1.26–1.63], $p<0.001$), and post-operative residual CE (aHR, 1.46 [95% CI 1.22–1.75], $p<0.001$) were independently associated with a shorter OS (Table 2). After adjustments using Cox models in the subgroup of patients with a contrast enhanced glioblastoma, surgical resection (aHR, 0.52 [95% CI 0.44–0.62], $p<0.001$) was independently associated with a longer OS, while age ≥ 70 years (aHR, 1.46 [95% CI 1.27–1.67], $p<0.001$), preoperative KPS score < 70 (aHR, 1.71 [95% CI 1.48–1.98], $p<0.001$), ring-like CE surrounding central necrosis (aHR, 1.20 [95% CI 1.01–1.42], $p=0.046$), tumour volume ≥ 30cm^3 (aHR, 1.41 [95% CI 1.23–1.60], $p<0.001$), and post-operative residual CE (aHR, 1.44 [95% CI 1.21–1.73], $p<0.001$) were independently associated with a shorter OS (Table 3).

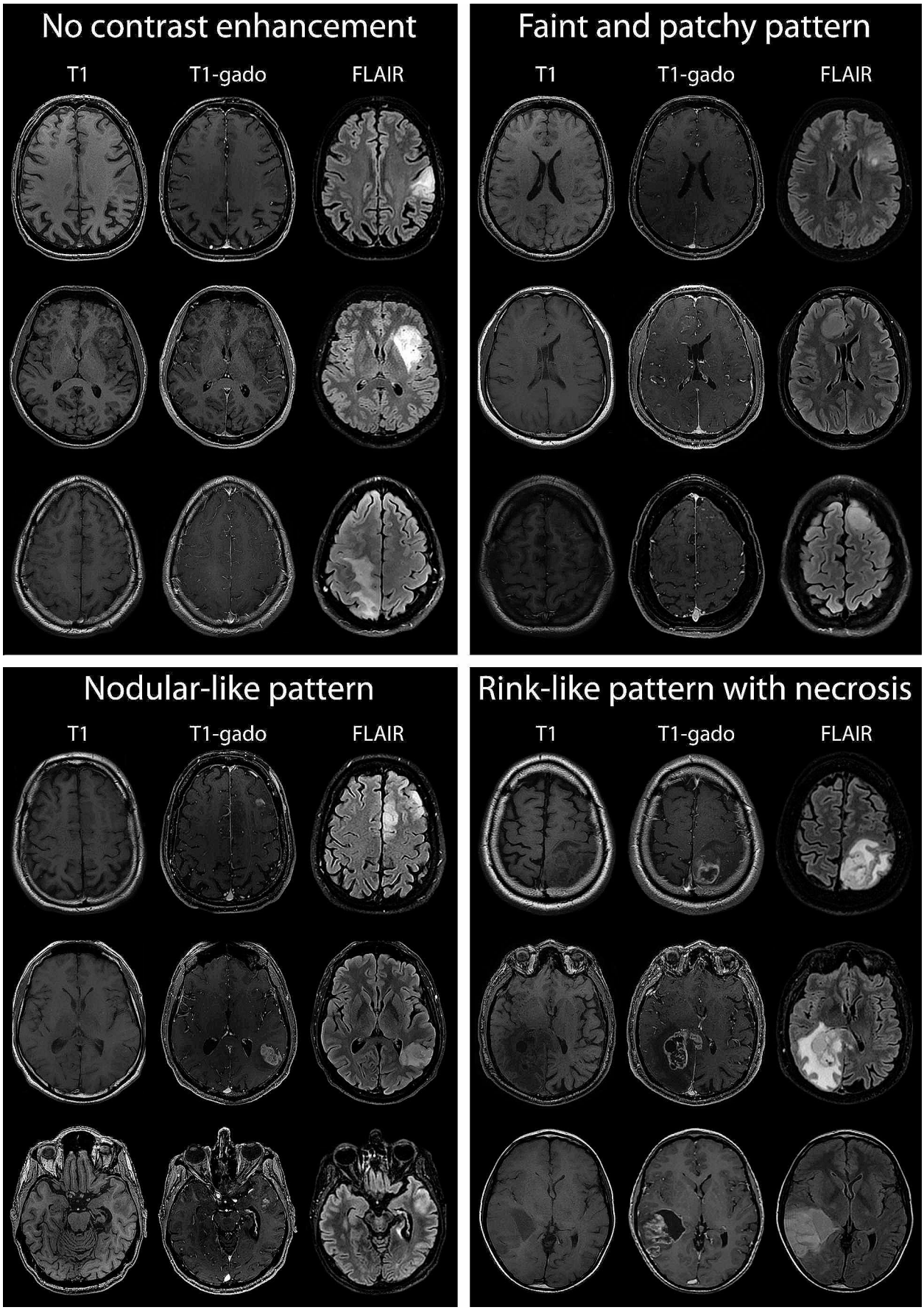
No contrast enhancement
T1
T1-gado
FLAIR
Faint and patchy pattern
T1
T1-gado
FLAIR
Nodular-like pattern
T1
T1-gado
FLAIR
Rink-like pattern with necrosis
T1
T1-gado
FLAIR

Discussion

Key results

In this retrospective, single-centre cohort study, we found that: (1) CE was typical in glioblastomas, *IDH*-wildtype, representing 97.7% of cases; (2) when present, the CE patterns were ring-like surrounding central necrosis in 85.5% of cases, nodular in 10.5% of cases, faint and patchy in 4.0% of cases; (3) non-contrast enhanced glioblastoma had a higher rate of long-term survivor than in contrast enhanced glioblastoma; (4) non-contrast enhanced glioblastomas had longer survivals while ring-like CE surrounding central necrosis glioblastomas had shorter survivals; (5) in contrast enhanced glioblastoma, surgical resection represents independent predictors of longer survivals, while age $\geq$ 70 years, preoperative KPS score < 70, tumour volume $\geq$ 30cm^3, and postoperative residual CE represent independent predictors of shorter survivals.

Interpretation

Contrast enhancement on MRI is a hallmark of glioblastoma, *IDH*-wildtype. This classical imaging description is challenged at the histo-molecular era: the diagnosis of glioblastoma can be made on non-enhanced tumour [23]. Non-contrast enhancing glioblastomas are defined by an abnormal signal intensity on FLAIR sequences without CE. Previous studies have suggested that non-contrast enhanced glioblastomas could be an early form of the disease [24–26]. A previous study identified this imaging subtype as "early-stage glioblastomas, *IDH*-wildtype" [9]. In 2018, the cIMPACT-NOW update 3 [23], integrated into the current 2021 WHO classification [1], defined the "diffuse astrocytic glioma *IDH*-wildtype with molecular features of glioblastoma". This entity described an astrocytoma, *IDH*-wildtype without morphological grade 4 criteria (i.e. microvascular proliferation and/or necrosis) but with molecular features of glioblastoma: *EGFR* amplification, combined gain of chromosome 7 and loss of chromosome 10, and/or *hTERT* promoter mutation [23]. However, this entity, regardless of its imaging findings, *de facto* integrates contrast-enhanced glioblastoma with a surgical sampling limited to the non-enhanced portion of the tumour, non-contrast enhanced glioblastoma with histopathological grade 4 criteria (i.e. microvascular proliferation and/or necrosis), or a non-optimal contrast injection procedure [9]. In the present study, we identified non-contrast enhanced glioblastoma, *IDH*-wildtype as a very rare entity, representing 2.3% of cases, with a better prognosis.

In diffuse gliomas, the CE patterns predict survival [12, 27]. In 2009, Pallud et al., identified the nodular-like pattern of CE and the time-progressive CE as predictors of worse OS in grade 2 gliomas [19]. In 2015, Wang et al., found that the presence of CE was associated with shorter PFS and OS in grade 3 anaplastic astrocytomas, *IDH*-mutant [28]. In 2017, Zhou et al., found that no CE and a smooth non-enhancing margin were predictive of longer PFS while a smooth non-enhancing margin was a significant predictor of longer OS in lower-grade gliomas [12]. Michiwaki et al. in 2019, found a 76.1% rate of ring-like CE surrounding central necrosis in glioblastomas, *IDH*-wildtype [29]. They found a high sensitivity (0.89) and specificity (0.91) of ring-like CE surrounding central necrosis to predict a glioblastoma, *IDH*-wildtype and identified this pattern of CE as a strong predictor of worse prognosis at the molecular era [29]. Similar than the present study, they showed that the ring-like CE surrounding central necrosis was the most frequent pattern of CE but did not assess the other CE patterns [29]. In 2020, Tesileanu et al. in a cohort of 268 newly diagnosed *IDH*-wildtype glioblastomas, found a rate of 7.4% of patients without contrast enhancement at diagnosis [14]. In 2023, Pokhylevych et al., found a 81.2% rate of ring-like CE surrounding central necrosis in paediatric glioblastomas [30]. A recent study assessed a cohort of 629 diffuse astrocytomas including *IDH*-mutant and *IDH*-wildtype subtypes and found a significant impact of CE and of CE pattern on survivals [9]. PFS and OS were both significantly longer in the non-enhancing tumour subgroup than in the faint and patchy CE pattern subgroup, and than in the nodular and ring-like CE surrounding central necrosis pattern subgroup [9]. They confirmed that the pattern of CE observed on preoperative MRI significantly impacted survival, and especially the ring-like CE surrounding central necrosis pattern, which was associated with worse OS [9]. Moreover, they performed a combined histo-radiological neoangiogenesis evaluation assessing the presence/absence of microvascular proliferation (MVP+/MVP-) based on histopathological analysis and the presence/absence of a CE (CE+/CE-) based on imaging analysis with a very high correlation between them (96.3%). The remaining cases had coherent explanations: focal MVP for CE-/MVP+ cases and presence of a marked perivascular lymphocytic inflammatory infiltrates and a gemistocytic component for CE+/MVP- cases. They demonstrated that adding preoperative and postoperative imaging analyses to the current histo-molecular diagnosis in daily clinical practice seems interesting and useful. However, all these studies were performed before the new 2021 WHO Classification of CNS Tumors. In the present study, we demonstrated similar results on glioblastomas, *IDH*-wildtype according to the latest 2021 WHO Classification, which suggests the usefulness of integrating the CE parameters that are easily available biomarkers in an integrated radio-histo-molecular grading system [9].

The present results also suggest the importance of analysing the early postoperative MRI in order to assess the representativity of the tumoral sampling and the presence of a residual CE [9]. Many recent studies highlighted the importance of

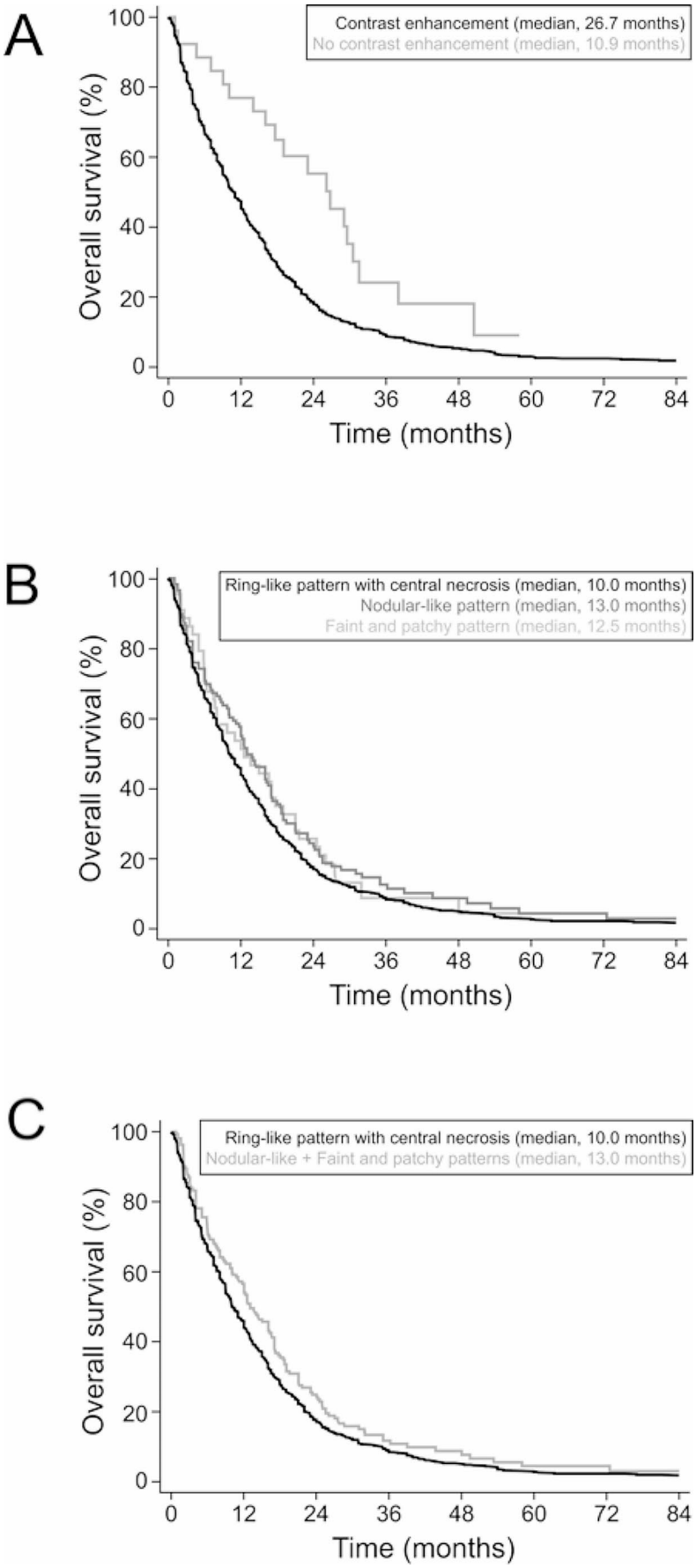

Fig. 2 Overall survival curves according to the Kaplan-Meier method
(**A**) The median OS was significantly higher in the non-contrast enhanced glioblastomas (26.7 months; 95%CI, 16.0-30.5) than in the contrast enhanced glioblastomas (10.9 months; 95%CI, 10.0–12.0) ($p < 0.001$). (**B**) In the subgroup of contrast enhanced glioblastomas ($n = 1123$, 97.7%), the median OS did not significantly differ between faint and patchy CE (12.5 months; 95%CI, 7.5–17.7), nodular CE (13.0 months; 95%CI, 10.7–16.5), and ring-like CE surrounding central necrosis (10.0 months; 95%CI, 9.4–11.2) ($p = 0.071$). (**C**) In the subgroup of contrast enhanced glioblastomas ($n = 1123$, 97.7%), the median OS was significantly shorter in ring-like CE surrounding central necrosis (10.0 months; 95%CI, 9.4–11.2) than in other patterns of CE (13.0 months; 95%CI, 11.0-16.2; $p = 0.033$)

Table 2 Predictors of overall survival in the whole series ($n = 1149$). Unadjusted and adjusted hazard ratios by Cox proportional hazards model

Parameters	Unadjusted Hazard Ratio			Adjusted Hazard Ratio		
	uHR	95% CI	*p*-value	aHR	95% CI	*p*-value
Clinical characteristics						
Sex						
Female	1 (ref)					
Male	1.07	0.95–1.21	0.258			
Age						
<70 years	1 (ref)			1 (ref)		
≥70 years	1.68	1.47–1.91	**< 0.001**	1.47	1.28–1.69	**< 0.001**
Preoperative Karnofsky Performance Status score						
≥70	1 (ref)			1 (ref)		
<70	2.01	1.74–2.32	**< 0.001**	1.72	1.48–1.99	**< 0.001**
Imaging characteristics						
Contrast enhancement						
No	1 (ref)			1 (ref)		
Yes	2	1.27–3.15	**0.003**	1.81	1.12–2.94	**0.015**
Tumour volume (cm^3), median 28.5cm^3						
<30 cm^3	1 (ref)			1 (ref)		
≥30 cm^3	1.31	1.16–1.48	**< 0.001**	1.44	1.26–1.63	**< 0.001**
Treatment-related characteristics						
Surgical treatment						
Biopsy	1 (ref)			1 (ref)		
Surgical resection	0.44	0.39–0.50	**< 0.001**	0.53	0.45–0.64	**< 0.001**
Extent of surgical resection						
Biopsy and partial resection	1 (ref)					
Subtotal, total and supratotal resection	0.44	0.38–0.49	**< 0.001**			
Post-operative residual contrast enhancement*						
No	1 (ref)			1 (ref)		
Yes	2.31	2.02–2.63	**< 0.001**	1.46	1.22–1.75	**< 0.001**

CI: confidence interval; uHR: unadjusted Hazard ratio; aHR: adjusted Hazard ratio; CE: contrast enhancement;

* No = total and supratotal resections; Yes = no-CE tumours, biopsy, partial and subtotal resection

accurately assess the extent of resection and the postoperative residual CE and non-CE volume [3, 31, 32].

Generalizability

We report a large study assessing the prognostic significance of CE on a single-centre, homogeneous cohort reflecting the real-life management of newly diagnosed supratentorial glioblastoma, *IDH*-wildtype in adults. We identified the presence of CE but also the pattern of CE as independent predictors of survivals (PFS and OS). Our results suggest incorporating these imaging criteria on the daily management of glioblastoma patients to refine their prognosis and management. In addition, we suggest incorporating CE parameters on future clinical trials as potential confounding factors. However, these results cannot be extrapolated to paediatric patients, to recurrent glioblastomas, *IDH*-wildtype and to other subtypes of high-grade gliomas (i.e. *IDH*-mutant, *H3K27M*-mutant, *H3G34*-mutant).

Limitations

The present results should be interpreted with caution given the retrospective, monocentric, and observational study design. We acknowledge the lack of systematic central imaging review for assessing the presence of CE and the pattern of CE (central imaging review performed in 46.6% of cases). The imbalance between the subgroup of non-contrast enhanced glioblastomas compared to contrast enhanced glioblastomas may have biased statistical analyses and precluded carrying statistical analyses on this subgroup and to study the impact of the extent of resection whose definition is different from the contrast enhanced glioblastomas [31]. Several variables of potential interest were not systematically collected in our dataset, including diffusion-weighted imaging (DWI), the dynamic susceptibility contrast perfusion-weighted imaging (DSC-PWI), the histopathological criteria (i.e. mitosis, necrosis and microvascular proliferation), and the *MGMT* promoter methylation status that may have impacted radiological and survival analyses. The lack of an external validation set also limited the generalizability of the results. Further confirmatory analyses are required.

Table 3 Predictors of overall survival in contrast enhanced glioblastoma patients ($n = 1123$). Unadjusted and adjusted hazard ratios by Cox proportional hazards model

Parameters	Unadjusted Hazard Ratio			Adjusted Hazard Ratio		
	uHR	95% CI	*p*-value	aHR	95% CI	*p*-value
Clinical characteristics						
Sex						
Female	1 (ref)					
Male	1.07	0.95–1.21	0.257			
Age						
<70 years	1 (ref)			1 (ref)		
≥70 years	1.68	1.47–1.92	**< 0.001**	1.46	1.27–1.67	**< 0.001**
Preoperative Karnofsky Performance Status score						
≥70	1 (ref)			1 (ref)		
<70	2.01	1.74–2.32	**< 0.001**	1.71	1.48–1.98	**< 0.001**
Imaging characteristics						
Pattern of contrast enhancement*						
Non necrotic	1 (ref)			1 (ref)		
Necrotic	1.2	1.01–1.44	**0.036**	1.2	1.01–1.42	**0.046**
Tumour volume (cm^3)						
<30 cm^3	1 (ref)			1 (ref)		
≥30 cm^3	1.31	1.16–1.48	**< 0.001**	1.41	1.23–1.60	**< 0.001**
Treatment-related characteristics						
Surgical treatment						
Biopsy	1 (ref)			1 (ref)		
Surgical resection	0.44	0.39–0.50	**< 0.001**	0.52	0.44–0.62	**< 0.001**
Extent of surgical resection						
Biopsy and partial resection	1 (ref)					
Subtotal, total and supratotal resection	0.42	0.37–0.47	**< 0.001**			
Post-operative residual contrast enhancement**						
No	1 (ref)			1 (ref)		
Yes	2.26	1.98–2.58	**< 0.001**	1.44	1.21–1.73	**< 0.001**

CI: confidence interval; uHR: unadjusted Hazard ratio; aHR: adjusted Hazard ratio; CE: contrast enhancement;

* Necrotic = ring-line CE surrounding necrosis; Non necrotic: faint and patchy CE and nodular CE

** No = total and supratotal resections; Yes = biopsy, partial and subtotal resection

Conclusion

The ring-like pattern of CE surrounding central necrosis is typical in glioblastomas, *IDH*-wildtype, representing 85.5% of cases, while the absence of CE is rare, representing 2.3% of cases. The presence/absence and pattern of CE in MRI are independent survival (OS) predictors in glioblastomas, *IDH*-wildtype. Further histo-molecular analyses are required to understand the differences in prognosis between non-contrast enhancing and contrast enhancing glioblastomas, *IDH*-wildtype in adults.

Supplementary Information The online version contains supplementary material available at https://doi.org/10.1007/s11060-024-04747-7.

Acknowledgements Alexandre Roux would like to thank the Nuovo-Soldati Foundation for Cancer Research, the Servier Institute and the Ligue contre le Cancer for their support.

Author contributions Alexandre Roux, Conception and design of the study, Acquisition and analysis of data, Drafting a significant portion of the manuscript or figures. Angela Elia, Acquisition and analysis of data, Drafting a significant portion of the manuscript or figures. Benoit Hudelist, Acquisition and analysis of data, Drafting a significant portion of the manuscript or figures. Joseph Benzakoun, Acquisition and analysis of data, Drafting a significant portion of the manuscript or figures. Edouard Dezamis, Acquisition and analysis of data, Drafting a significant portion of the manuscript or figures. Eduardo Parraga, Acquisition and analysis of data, Drafting a significant portion of the manuscript or figures. Alessandro Moiraghi, Acquisition and analysis of data, Drafting a significant portion of the manuscript or figures. Giorgia Antonia Simboli, Acquisition and analysis of data, Drafting a significant portion of the manuscript or figures. Fabrice Chretien, Acquisition and analysis of data, Drafting a significant portion of the manuscript or figures. Catherine Oppenheim, Acquisition and analysis of data, Drafting a significant portion of the manuscript or figures. Marc Zanello, Conception and design of the study, Drafting a significant portion of the manuscript or figures. Johan Pallud, Conception and design of the study, Acquisition and analysis of data, Drafting a significant portion of the manuscript or figures.

Funding The authors declare that no funds, grants, or other support were received during the preparation of this manuscript.

Data availability No datasets were generated or analysed during the current study.

Declarations

Ethics approval The study received required authorizations (IRB#1:2024/13) from the human research institutional review board (IRB00011687).

Consent to participate Informed consent was obtained from all individual participants included in the study. The requirement to obtain informed consent was waived according to French legislation (observational retrospective study).

Consent to publish The authors affirm that human research participants provided informed consent for publication of the images in Fig. 1.

Competing interests The authors declare no competing interests.

Previous presentation No portion of the present content has been previously presented.

References

1. Louis DN, Perry A, Wesseling P et al (2021) The 2021 WHO classification of tumors of the central nervous system: a summary. Neuro-Oncol 23:1231–1251. https://doi.org/10.1093/neuonc/noab106
2. Sanai N, Polley M-Y, McDermott MW et al (2011) An extent of resection threshold for newly diagnosed glioblastomas. J Neurosurg 115:3–8. https://doi.org/10.3171/2011.2.JNS10998
3. Chaichana KL, Jusue-Torres I, Navarro-Ramirez R et al (2014) Establishing percent resection and residual volume thresholds affecting survival and recurrence for patients with newly diagnosed intracranial glioblastoma. Neuro-Oncol 16:113–122. https://doi.org/10.1093/neuonc/not137
4. Marko NF, Weil RJ, Schroeder JL et al (2014) Extent of resection of glioblastoma revisited: personalized survival modeling facilitates more accurate survival prediction and supports a maximum-safe-resection approach to surgery. J Clin Oncol off J Am Soc Clin Oncol 32:774–782. https://doi.org/10.1200/JCO.2013.51.8886
5. Roux A, Peeters S, Zanello M et al (2017) Extent of resection and carmustine wafer implantation safely improve survival in patients with a newly diagnosed glioblastoma: a single center experience of the current practice. J Neurooncol. https://doi.org/10.1007/s11060-017-2551-4
6. Molinaro AM, Hervey-Jumper S, Morshed RA et al (2020) Association of maximal extent of resection of contrast-enhanced and non-contrast-enhanced tumor with survival within molecular subgroups of patients with newly diagnosed glioblastoma. JAMA Oncol. https://doi.org/10.1001/jamaoncol.2019.6143
7. Moiraghi A, Roux A, Peeters S et al (2021) Feasibility, safety and impact on overall survival of awake resection for newly diagnosed supratentorial IDH-wildtype glioblastomas in adults. Cancers 13:2911. https://doi.org/10.3390/cancers13122911
8. Stupp R, Mason WP, van den Bent MJ et al (2005) Radiotherapy plus concomitant and adjuvant temozolomide for glioblastoma. N Engl J Med 352:987–996. https://doi.org/10.1056/NEJMoa043330
9. Roux A, Tran S, Edjlali M et al (2020) Prognostic relevance of adding MRI data to WHO 2016 and cIMPACT-NOW updates for diffuse astrocytic tumors in adults. Working toward the extended use of MRI data in integrated glioma diagnosis. Brain Pathol Zurich Switz e12929. https://doi.org/10.1111/bpa.12929
10. Delfanti RL, Piccioni DE, Handwerker J et al (2017) Imaging correlates for the 2016 update on WHO classification of grade II/III gliomas: implications for IDH, 1p/19q and ATRX status. J Neurooncol 135:601–609. https://doi.org/10.1007/s11060-017-2613-7
11. Guo H, Kang H, Tong H et al (2019) Microvascular characteristics of lower-grade diffuse gliomas: investigating vessel size imaging for differentiating grades and subtypes. Eur Radiol 29:1893–1902. https://doi.org/10.1007/s00330-018-5738-y
12. Zhou H, Vallières M, Bai HX et al (2017) MRI features predict survival and molecular markers in diffuse lower-grade gliomas. Neuro-Oncol 19:862–870. https://doi.org/10.1093/neuonc/now256
13. Hempel J-M, Brendle C, Bender B et al (2018) Contrast enhancement predicting survival in integrated molecular subtypes of diffuse glioma: an observational cohort study. J Neurooncol 139:373–381. https://doi.org/10.1007/s11060-018-2872-y
14. Tesileanu CMS, Dirven L, Wijnenga MMJ et al (2020) Survival of diffuse astrocytic glioma, IDH1/2 wildtype, with molecular features of glioblastoma, WHO grade IV: a confirmation of the cIMPACT-NOW criteria. Neuro-Oncol 22:515–523. https://doi.org/10.1093/neuonc/noz200
15. Daumas-Duport C, Monsaigneon V, Blond S et al (1987) Serial stereotactic biopsies and CT scan in gliomas: correlative study in 100 astrocytomas, oligo-astrocytomas and oligodendrocytomas. J Neurooncol 4:317–328. https://doi.org/10.1007/bf00195602
16. Pons-Escoda A, Majos C, Smits M, Oleaga L (2024) Presurgical diagnosis of diffuse gliomas in adults: Post-WHO 2021 practical perspectives from radiologists in neuro-oncology units. Radiol Engl Ed. https://doi.org/10.1016/j.rxeng.2024.03.002
17. Stupp R, Hegi ME, Mason WP et al (2009) Effects of radiotherapy with concomitant and adjuvant temozolomide versus radiotherapy alone on survival in glioblastoma in a randomised phase III study: 5-year analysis of the EORTC-NCIC trial. Lancet Oncol 10:459–466. https://doi.org/10.1016/S1470-2045(09)70025-7
18. vonelm2007.pdf
19. Pallud J, Capelle L, Taillandier L et al (2009) Prognostic significance of imaging contrast enhancement for WHO grade II gliomas. Neuro-Oncol 11:176–182. https://doi.org/10.1215/15228517-2008-066
20. Roux A, Roca P, Edjlali M et al (2019) MRI atlas of IDH wild-type supratentorial glioblastoma: probabilistic maps of phenotype, management, and outcomes. Radiology 293:633–643. https://doi.org/10.1148/radiol.2019190491
21. Vogelbaum MA, Jost S, Aghi MK et al (2012) Application of novel response/progression measures for surgically delivered therapies for gliomas: response assessment in neuro-oncology (RANO) working group. Neurosurgery 70:234–243 discussion 243–244. https://doi.org/10.1227/NEU.0b013e318223f5a7
22. Lacroix M, Abi-Said D, Fourney DR et al (2001) A multivariate analysis of 416 patients with glioblastoma multiforme: prognosis, extent of resection, and survival. J Neurosurg 95:190–198. https://doi.org/10.3171/jns.2001.95.2.0190
23. Brat DJ, Aldape K, Colman H et al (2018) cIMPACT-NOW update 3: recommended diagnostic criteria for diffuse astrocytic glioma, IDH-wildtype, with molecular features of glioblastoma, WHO grade IV. Acta Neuropathol (Berl) 136:805–810. https://doi.org/10.1007/s00401-018-1913-0
24. Ideguchi M, Kajiwara K, Goto H et al (2015) MRI findings and pathological features in early-stage glioblastoma. J Neurooncol 123:289–297. https://doi.org/10.1007/s11060-015-1797-y

25. Faguer R, Tanguy J-Y, Rousseau A et al (2014) Early presentation of primary glioblastoma. Neurochirurgie 60:188–193. https://doi.org/10.1016/j.neuchi.2014.02.008
26. Hishii M, Matsumoto T, Arai H (2019) Diagnosis and treatment of early-stage glioblastoma. Asian J Neurosurg 14:589–592. https://doi.org/10.4103/ajns.AJNS_18_19
27. Juratli TA, Tummala SS, Riedl A et al (2019) Radiographic assessment of contrast enhancement and T2/FLAIR mismatch sign in lower grade gliomas: correlation with molecular groups. J Neurooncol 141:327–335. https://doi.org/10.1007/s11060-018-03034-6
28. Wang YY, Wang K, Li SW et al (2015) Patterns of tumor contrast enhancement predict the prognosis of anaplastic gliomas with IDH1 mutation. AJNR Am J Neuroradiol 36:2023–2029. https://doi.org/10.3174/ajnr.A4407
29. Michiwaki Y, Hata N, Mizoguchi M et al (2019) Relevance of calcification and contrast enhancement pattern for molecular diagnosis and survival prediction of gliomas based on the 2016 World Health Organization classification. Clin Neurol Neurosurg 187:105556. https://doi.org/10.1016/j.clineuro.2019.105556
30. Pokhylevych H, Khose S, Gule-Monroe MK et al (2023) Contrast enhancement patterns in pediatric glioblastomas. J Comput Assist Tomogr 47:115–120. https://doi.org/10.1097/RCT.0000000000001379
31. Karschnia P, Young JS, Dono A et al (2023) Prognostic validation of a new classification system for extent of resection in glioblastoma: a report of the RANO resect group. Neuro-Oncol 25:940–954. https://doi.org/10.1093/neuonc/noac193
32. Karschnia P, Dietrich J, Bruno F et al (2024) Surgical management and outcome of newly diagnosed glioblastoma without contrast enhancement (low-grade appearance): a report of the RANO resect group. Neuro-Oncol 26:166–177. https://doi.org/10.1093/neuonc/noad160